A Project Report on

Decision-Directed MMSE Receiver in LTE Downlink

Submitted by

Amrit Vohra

in partial fulfilment of the requirements

for the award of degree of

Master of Technology

DEPARTMENT OF ELECTRICAL ENGINEERING

INDIAN INSTITUTE OF TECHNOLOGY MADRAS

May 2013

THESIS CERTIFICATE

This is to certify that the thesis titled **Decision-Directed MMSE Receiver for LTE Downlink**, submitted by **Amrit Vohra**, to the Indian Institute of Technology, Madras, for the award of the degree of **Master of Technology**, is a bona fide record of the research work done by him under our supervision. The contents of this thesis, in full or in parts, have not been submitted to any other Institute or University for the award of any degree or diploma.

Dr. K Giridhar
Project Guide
Professor
Dept. of Electrical Engineering
IIT-Madras, 600 036

Dr. Sheetal Kalyani
Project Co-Guide
Assistant Professor
Dept. of Electrical Engineering
IIT-Madras, 600 036

Place: Chennai

Date: 2013

Acknowledgements

I would like to express my humble gratitude and thankfulness to Dr. K Giridhar and Dr. Sheetal Kalyani for their kind encouragement, freedom and patient guidance through the course of this project. It was indeed a wonderful experience to learn the challenges in research, discuss ideas, gain insight on the topic of my project work. I feel honoured and encouraged to have worked under their guidance. I am also deeply indebted to the Department of Electrical Engineering for all the interesting courses that I have completed. I am also extremely grateful to the Heads of the Department - Dr. Enakshi Bhattacharya, Faculty Advisor - Dr David R Koilpillai, and all other faculty members with whom I interacted directly or indirectly for their continuous guidance and support during the respective courses and also in general.

I am also thankful to the non faculty members of the department of EE, especially the office staff who always extended their valuable support in all my endeavours. I also want to express my gratitude to all my lab mates for their continuous guidance & course correction and for making the lab a place for learning with fun.

I would also like to immensely thank my organisation, Indian Navy for giving me this opportunity to pursue my Post Graduation at this prestigious institution. It is my pleasure to make a special thanks to my dearest wife & kid, parents, classmates and friends who have made this a memorable endeavour indeed. Lastly, nothing would have been possible without the blessings and kindness of Almighty God and his ubiquitous influence and guidance at each step.

Abstract

In multi-cell orthogonal frequency division multiple access (OFDMA) systems employing frequency reuse-1, the received signals of the cell edge users have a very low signal-to-interference-noise-ratio (SINR) due to co channel interference (CCI) from neighboring cells/sectors.The interference rejection combining (IRC) receiver is effective in improving the cell-edge user throughput because it suppresses inter-cell interference. The IRC receiver is typically based on the minimum mean square error (MMSE) criteria, which requires channel estimation and interference-plus-noise covariance matrix estimation including the inter-cell interference with high accuracy. The covariance matrix is evaluated by averaging covariance matrices obtained at 08 reference signal (RS) points scattered within a resource block (RB). In this thesis, we propose two decision directed (DD) schemes which are based on inclusion of decisions made (data points) in estimating the covariance matrix.

In first scheme, single DD covariance matrix is formed and in the second scheme, multiple (one for each subcarrier) DD covariance matrices are formed. Also a method for adaptively choosing between these two DD schemes is proposed, which is based on correlation factor of channel coherence bandwidth. The performance of RS based covariance matrix estimation scheme, single DD covariance matrix estimation scheme, multiple DD covariance matrices estimation scheme has been investigated under varying channel conditions, modulation schemes, interferer source power levels and number of interfering sources.

Contents

List of Figures

List of Tables

1 Introduction

MIMO communications have been intensely studied over the last few years and widely considered as a suitable way to improve performances of a modern wireless communications. MIMO scheme can be split in two categories: space time coding (STC) and spatial multiplexing (SM). STC improves the reliability of the communication system, while SM achieves a higher data rate by transmitting independent data streams on the different antennas simultaneously. With a maximum-likelihood (ML) detection, SM scheme has the maximum receive diversity order. The disadvantage of the ML detection is the high computational complexity. A complexity reduction can be obtained by applying linear zero-forcing (ZF) or minimum mean square error (MMSE) receiver.

The type of receiver employed at user equipment (UE) in LTE downlink is IRC receiver which is typically based on MMSE and is effective in improving the cell-edge user throughput. The IRC receiver utilises the correlation of the interference of multiple receiver branches, and combines the received signals for multiple receiver branches so that the mean square error (MSE) between the combined signal and the desired signal is minimised. However, the IRC receiver requires the knowledge of interference signals, i.e. the interference-plus-noise covariance matrix including the interference signals, in addition to the desired signal. Therefore, the IRC receiver is sensitive to not only channel estimation error but also covariance matrix estimation error. The inspiration of present work is to accurately determining interference-plus-noise covariance matrix. It is assumed in our work that channel

is perfectly known at the receiver.

The covariance matrix is evaluated by averaging covariance matrices obtained at 08 RS points scattered within a RB. In this thesis, we propose two DD schemes which are based on inclusion of decisions made (data points) in calculating the covariance matrix. In the first scheme, single DD covariance matrix is formed and in the second scheme, multiple (one for each subcarrier) DD covariance matrices are formed. Also a method for adaptively choosing between these two DD schemes is proposed, which is based on correlation factor of channel coherence bandwidth. Simulations are performed to compare performance of RS based covariance matrix scheme, single DD covariance matrix scheme, Multiple covariance matrices DD scheme and the adaptive scheme under varying channel conditions, modulation schemes, interferer source power levels and number of interfering sources.

Flow of thesis:

The thesis is organised as follows:

Chapter 2 provides the theoretical background of OFDM which is a high data rate wireless communication technique. It also presents an overview of physical layer of long term evolution (LTE).

Chapter 3 presents various standard parameter used in LTE downlink physical layer. It also provides various standard channel models used in LTE. Further, it discusses basic principle of MIMO IRC receiver used in LTE downlink at UE.

Chapter 4 presents the new proposed scheme based on decision-directed covariance matrix evaluation. It also provides simulation results, which compare the symbol error rate (SER)/ block error rate (BLER) performance of conventional IRC receiver and the DD based receiver for various channel models and modulation schemes.

Chapter 5 gives the conclusion of our work.

2 Basics and Background

2.1 OFDM

The ever growing demand of high data rates wireless transmission has stimulated interest in multicarrier modulation schemes. As the data rate is increased, the system using single carrier modulation suffers from sever inter symbol interference (ISI) caused by the dispersive fading of wireless channels. OFDM is a multicarrier modulation scheme which divides the entire frequency selective fading channel into many narrow band flat fading sub-channels in which high-bit-rate data are transmitted in parallel and do not undergo ISI due to the long symbol duration.

OFDM modulation has been chosen for many standards, including Digital Audio Broadcasting (DAB) and terrestrial TV in Europe, and wireless local area network (WLAN). Moreover, it is also an important technique for high data-rate transmission over mobile wireless channels and therefore is used in IEEE 802.16 and 4G standards.

2.1.1 Data Transmission in OFDM

An OFDM signal consists of a sum of sub-carriers that are modulated by using phase shift keying (PSK) or quadrature amplitude modulation (QAM). If d_i is the complex QAM symbol, N_s is the number of sub-carriers, T the symbol duration, and $f_i = f_o + \frac{i}{T}$ the carrier frequency, then one OFDM symbol starting at $t = t_s$

can be written as:

$$s(t) = Re\left\{\sum_{i=0}^{N_s-1} d_i\, exp(j2\pi f(t-t_s))\right\},\ t_s \leq t \leq t_s + T \tag{2.1}$$

The equivalent complex notation of the OFDM symbol is as follows:

$$s(t) = \sum_{i=0}^{N_s-1} d_i\, exp(j2\pi f(t-t_s)),\ t_s \leq t \leq t_s + T \tag{2.2}$$

In this representation, the real and imaginary parts correspond to the in-phase and quadrature parts of the OFDM signal, which have to be multiplied by a cosine and sine of the desired carrier frequency to produce final OFDM signal. Figure (2.1) shows the block diagram of OFDM modulator.

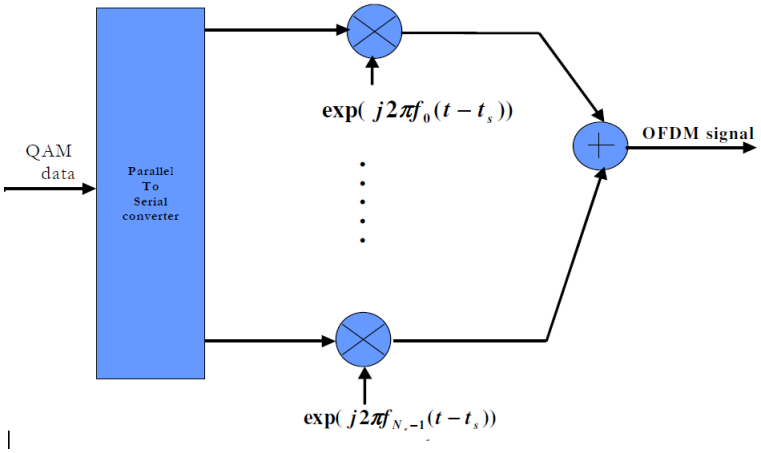

Figure 2.1: OFDM Modulator

To further get the insight of the OFDM modulation, let us consider an OFDM symbol comprising of four sub-carriers as shown in figure (2.2). We can observe that all the sub-carriers have the same phase and amplitude, but in practice the amplitudes and phases may be modulated differently for each sub-carrier. It is worth noting that each sub-carrier has exactly integer number of cycles in the in-

terval T, and the number of cycles between adjacent sub-carriers differs by exactly one. This property accounts for the orthogonality between sub-carriers.

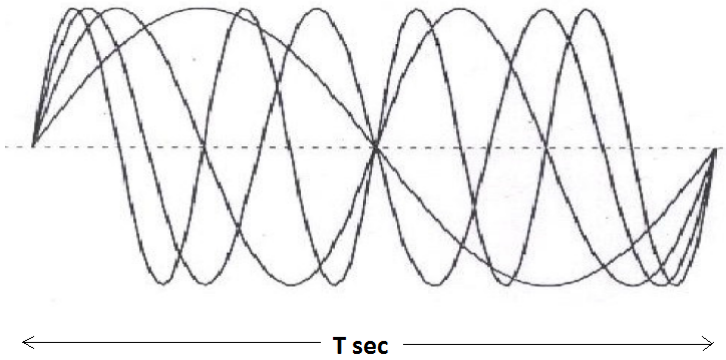

Figure 2.2: OFDM Sub-carriers

Each OFDM symbol contains sub-carriers that are non-zero over a Tseconds interval. Hence, the spectrum of a single symbol is a convolution of group of Dirac pulses located at the sub-carrier frequencies with the spectrum of a square pulse that is one for a Tseconds period and zero otherwise. The amplitude spectrum of a square pulse is equal to $sinc(\pi ft)$, which has zeros for all frequencies f that are an integer multiple of $1/T$. This effect is shown in figure (2.3) which shows overlapping sinc spectra of individual sub-carriers. At the maximum of each sub-carrier spectrum, all other sub-carrier spectra are zero. Thus, at maxima, each sub-carrier is free from any interference from other sub-carriers. Therefore, instead of ISI, it is inter carrier interference (ICI) that is avoided by maintaining the orthogonality among sub-carriers.

The complex baseband signal as defined by (Equation 2.2) is nothing but the inverse Fourier transform of N_s QAM symbols. The time discrete equivalent is the inverse discrete Fourier transform (IDFT), which is given by:

$$s(n) = \sum_{i=0}^{N_s-1} d_i \, exp(j2\pi \frac{in}{N}) \tag{2.3}$$

Where the time t is replaced by a sample number n. In practice, this transform

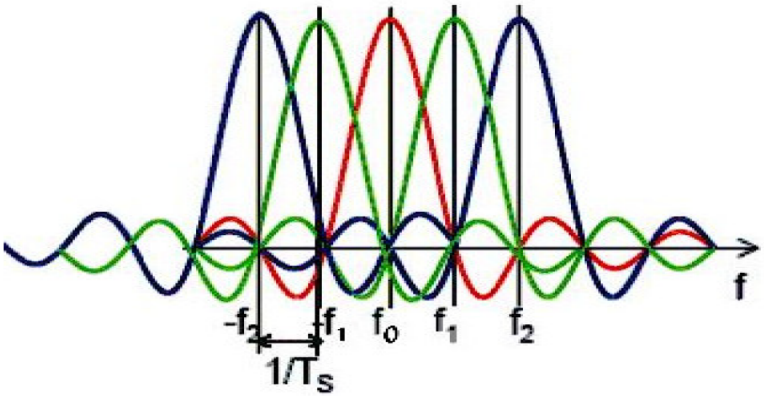

Figure 2.3: Sub-carriers overlapping

can be implemented very efficiently by the inverse Fast Fourier Transform (IFFT). The demodulation OFDM symbol at the receiver is performed using Fast Fourier Transform (FFT).

2.1.2 Guard Time and Cyclic Prefix

One of the most important reasons to do OFDM is the efficient way it deals with multipath delay spread. By dividing the input data stream in N_s sub-carriers, the symbol duration of each sub-carrier is made $N_s$times larger and thus becomes significantly longer than channel delay spread. To eliminate ISI almost completely, a guard time is introduced for each OFDM symbol. The guard time is chosen larger than the expected delay spread, such that the multipath components from one symbol cannot interfere with the next symbol. In order to maintain the orthogonality among the sub-carriers, the OFDM symbols are cyclically extended i.e the delayed replicas of the OFDM symbols are prefixed to the symbol. This ensures integer number of cycles within the FFT interval, as long as the delay is lesser than the guard time. As a result, multipath signals with delays smaller than the guard time cannot cause ICI. The respective block diagram of OFDM transmitter and receiver are shown in figure 2.4 and 2.5.

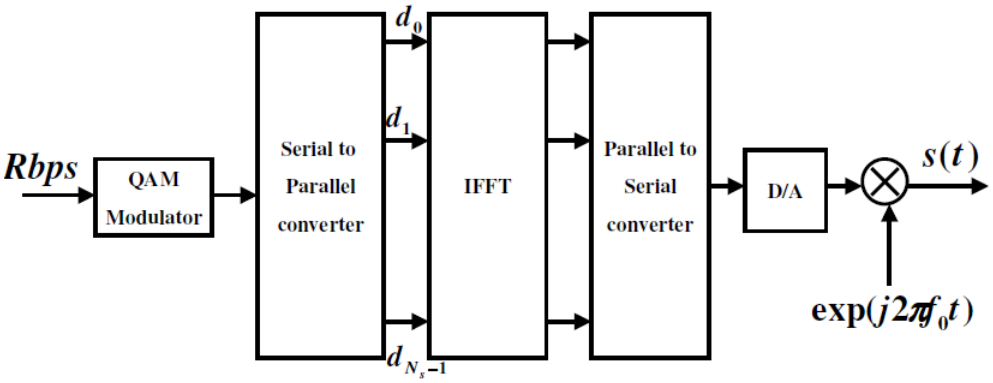

Figure 2.4: OFDM Transmitter

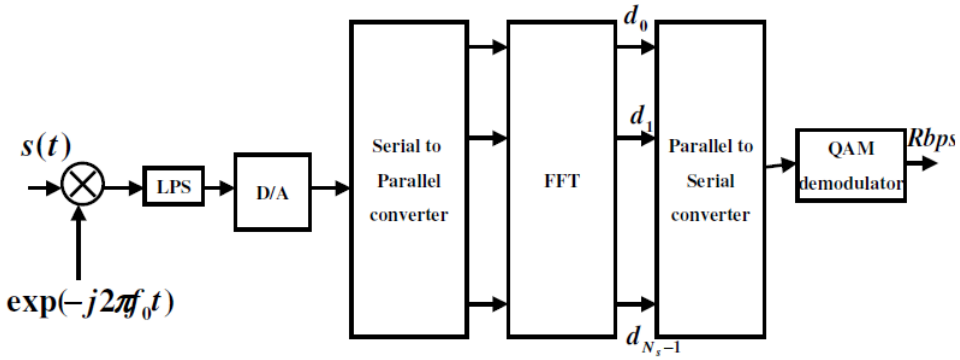

Figure 2.5: OFDM Receiver

2.2 3GPP Long Term Evolution

In order to cope with the ever growing demand for packet-based mobile data communication and to meet the needs of future mobile communications, 3GPP (3rd Generation Partnership Project) has standardised a new technology called LTE as the next step of the current 3G mobile networks. LTE is a 4th generation wireless network technology based on OFDM and multiple input multiple output (MIMO). Key features of LTE are as follows:

- Supports peak data rates of up to 100 Mbps on the downlink and 50 Mbps on the uplink when using a 20 MHz channel bandwidth.
- Improves spectrum efficiency by employing OFDM and MIMO.
- Employs both types of spectrum allocations i.e frequency division duplex (FDD) and time division duplex (TDD).

- Supports scalable RF channel bandwidths. Allowed values are 1.4, 3, 5, 10, 15 and 20 MHz.
- Inter-operates with W-CDMA and GSM systems and non-3GPP systems.

2.2.1 LTE Physical Layer Overview

The design of LTE physical layer is mainly influenced by the requirements for high data rates, spectral efficiency and multiple channel bandwidths. In order to fulfil these requirements, OFDM was selected as the basis for the PHY layer. In addition to OFDM, LTE implements multiple antenna techniques such as MIMO which can either increase channel capacity (by spatial multiplexing) or enhance signal robustness (space frequency/time coding). LTE uses OFDMA for downlink transmission and single carrier frequency division multiple access (SCFDMA) for uplink transmission.

2.2.1.1 Downlink Transmission

LTE uses OFDMA, which uses OFDM as a multi-carrier scheme that allocates radio resources to multiple users. For LTE, OFDM splits the carrier frequency bandwidth into many small sub-carriers spaced at 15 KHz, and then modulates each individual sub-carrier using the QPSK, 16-QAM or 64-QAM digital modulation formats. OFDMA allows sharing of available bandwidth by multiple users at the same time. OFDMA assigns each user the bandwidth needed for their transmission. Unassigned sub-carriers remain off, thus reducing power consumption and interference.

2.2.1.2 Uplink Transmission

In the uplink, LTE uses a pre-coded version of OFDM called SC-FDMA. SC-FDMA has a lower PAPR (Peak-to-Average Power Ratio) than OFDM. This lower

PAPR reduces battery power consumption, requires a simpler amplifier design and improves uplink coverage and cell-edge performance. In SC-FDMA, the data spreads across multiple sub-carriers, unlike OFDMA where each sub-carrier transports unique data. The need for a complex receiver makes SC-FDMA unacceptable for downlink. The difference between OFDM and SC-FDMA is depicted in figure 2.6.

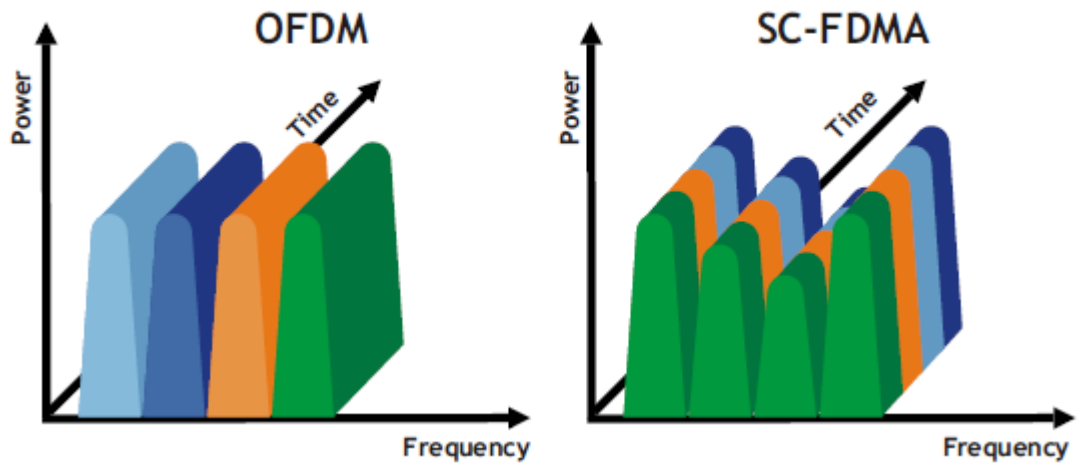

Figure 2.6: OFDMA vs SC-FDMA

2.2.1.3 Adaptive Modulation and Coding

Adaptive Modulation and Coding refers to the ability of the network to determine the modulation type and the coding rate dynamically based on the current RF channel conditions reported by the UE in channel state feedback reports. The most important part of this feedback is channel quality indicator (CQI) which indicates the link adaptation parameters that the UE can support in that time/ channel realisation. The RF digital modulation schemes that are used in LTE to modulate the information are QPSK, 16-QAM, and 64-QAM. In QPSK, there are four possible symbol states and each symbol carries two bits of information. In 16-QAM, there are 16 symbol states. Each 16-QAM symbol carries 4 bits. In 64-QAM, there are 64 symbol states. Each 64-QAM symbol carries 6 bits. Higher-

order modulation is more sensitive to poor channel conditions than the lower-order modulation because the detector in the receiver must resolve smaller differences as the constellations become more dense.

Coding refers to an error-correction methodology that adds extra bits to the data stream that allow error correction. Specified as fractions, Code Rates specify the number of data bits in the numerator and the total number of bits in the denominator. Thus if the Code Rate is 1/3, protection bits are added so one bit of data is sent as three bits. The mother code rate in LTE is 1/3.

3 LTE Downlink Overview and MMSE Receiver

LTE downlink uses OFDMA for resource allocation to UEs. The resources are allocated to users in time and frequency. The LTE downlink parameters are given in table 3.1.

Channel Bandwidth (MHz)	1.25	2.5	5	10	15	20
Frame Duration (ms)	10					
Subframe Duration (ms)	1					
Sub-carrier Spacing (kHz)	15					
Sampling Frequency (MHz)	1.92	3.84	7.68	15.36	23.04	30.72
FFT Size	128	256	512	1024	1536	2048
Occupied Sub-carriers (inc. DC sub-carrier)	76	151	301	601	901	1201
Guard Sub-carriers	52	105	211	423	635	847
Number of Resource Blocks	6	12	25	50	75	100
Occupied Channel Bandwidth (MHz)	1.140	2.265	4.515	9.015	13.515	18.015
DL Bandwidth Efficiency	77.1%	90%	90%	90%	90%	90%
OFDM Symbols/Subframe	7/6 (short/long CP)					
CP Length (Short CP) (μs)	5.2 (first symbol) / 4.69 (six following symbols)					
CP Length (Long CP) (μs)	16.67					

Table 3.1: LTE downlink parameters

3.1 Frame Structure

Two types of radio frame structures are designed for LTE: Type-1 frame structure is applicable to FDD and type-2 frame structure is related to TDD.

3.1.1 Type-1 Frame Structure

Type-1 frame structure is designed for frequency division duplex and is valid for both half duplex and full duplex FDD modes. Type-1 radio frame has a duration 10 ms and consists of equally sized 20 slots each of 0.5 ms numbered from 0 to 19. A subframe comprises two slots, thus one radio frame has 10 subframes as illustrated in figure 3.1. Channel dependent scheduling and link adaptation operate on a subframe level. In FDD mode, half of the sub-frames are available for downlink and the other half are available for uplink transmission in each 10 ms interval, where downlink and uplink transmission are separated in the frequency domain.

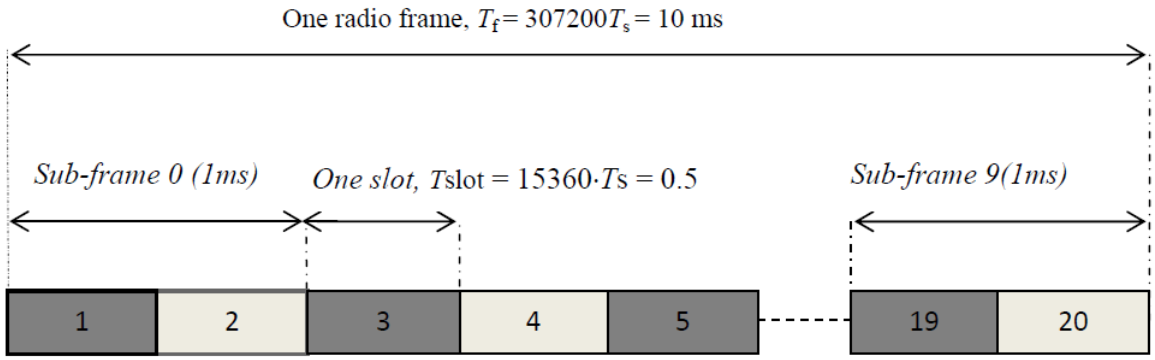

Figure 3.1: Type-1 Frame structure (T_s is expressing basic time unit corresponding to 30.72MHz)

Each slot consists of a number of OFDM symbols including cyclic prefix (CP). CP is a kind of guard interval to combat inter-OFDM-symbol interference, which should be larger than the channel delay spread. Therefore, the length of CP depends on the environment where the network operates, and it should not be too large as it brings a bandwidth and power penalty. With a subcarrier spacing $\Delta f = 15KHz$, the OFDM symbol time is $66.7\mu s$. As shown in figure 3.2, LTE defines two different CP lengths: a normal CP and an extended CP, corresponding to seven and six OFDM symbols per slot, respectively.

The extended CP is for multicell broadcast and very-large-cell scenarios with large delay spread at a price of bandwidth efficiency, with length $T_{eCP} = 512.Ts \approx 16.7$. The normal CP is suitable for urban environment and high data rate applications.

Note that the normal CP lengths are different for the first ($T_{CP} = 160.Ts \approx 5.2\mu s$) and subsequent OFDM symbols ($T_{CP} = 144.Ts \approx 4.7\mu s$), which is to fill the entire slot of 0.5 ms. The numbers of CP samples for different bandwidths are shown in Table 3.1. For example, with 10MHz bandwidth, the sampling time is 1/(15000 × 1024) sec and the number of CP samples for the extended CP is 256, which provides the required CP length of 256/(15000×1024) ≈1.67μs. In case of 7.5kHz subcarrier spacing, there is only a single CP length, corresponding to 3 OFDM symbols per slot.

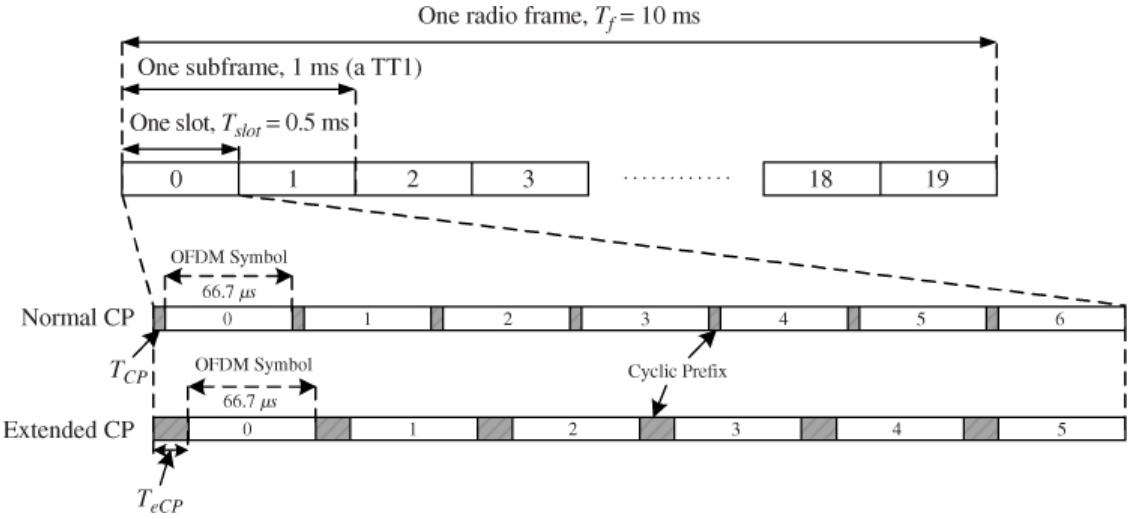

Figure 3.2: Type 1 frame - normal and extended CP

3.1.2 Type-2 Frame Structure

Type 2 frame structure is relevant for TDD; the radio frame is composed of two identical half frames each one having duration of 5ms. Each half frame is further divided into 5 sub frames having duration of 1ms as demonstrated in figure 3.3. Two slots of length 0.5ms constitute a sub frame which is not special sub frame. The special type of sub frames is composed of three fields Downlink Pilot Timeslot (DwPTS), GP (Guard Period) and Uplink Pilot Timeslot (UpPTS). Seven uplink-downlink configurations are supported with both types (10ms and 5ms) of downlink to uplink switch point periodicity. In 5m downlink to uplink

switch point periodicity, special type of sub frames are used in both half frames but it is not the case in 10ms downlink to uplink switch point periodicity, special frame are used only in first half frame. For downlink transmission sub frames 0, 5 and DwPTS are always reserved. UpPTS and the sub frame next to the special sub frame are always reserved for uplink communication.

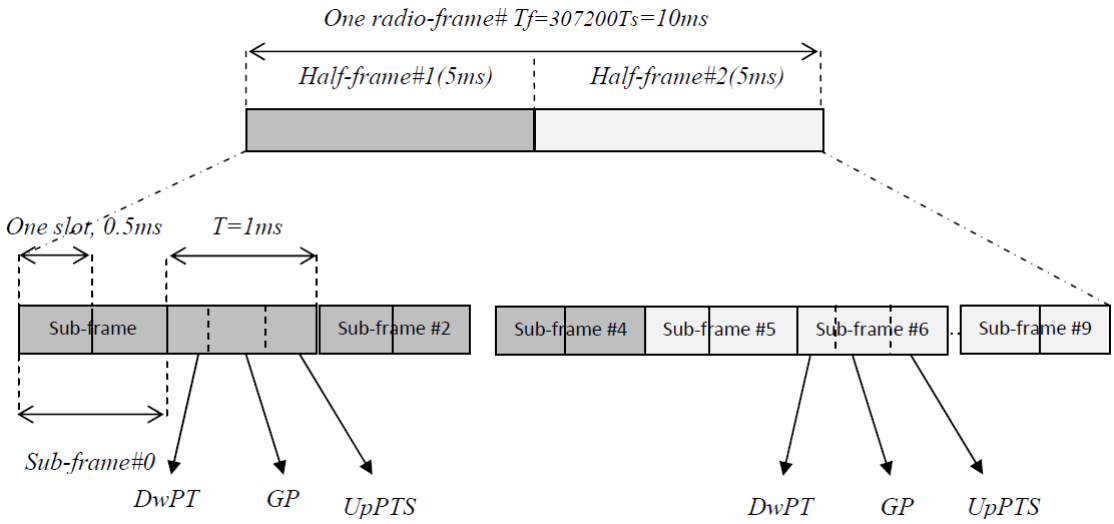

Figure 3.3: Frame structure type 2 (for 5 ms switch point periodicity)

3.2 Slot Structure and Resource Allocation

In each available slot the transmitted signal can be seen as a time-frequency recourse grid. Each column and each row of the resource grid correspond to one OFDM symbol and one OFDM subcarrier respectively. A Resource Element (RE) is the smallest defined unit which consists of one OFDM sub-carrier during one OFDM symbol interval. The number of sub carriers is being determined by the transmission bandwidth. For normal cyclic prefix (CP) each slot contains seven OFDM symbols and in case of extended cyclic prefix, 6 OFDM symbols are slotted in each time slot. The different lengths of CP are mention in Table 2.1. In this work we have used only normal CP length with Type 1 frame structure.

In LTE downlink, a constant sub carriers spacing of 15 kHz is used. In frequency

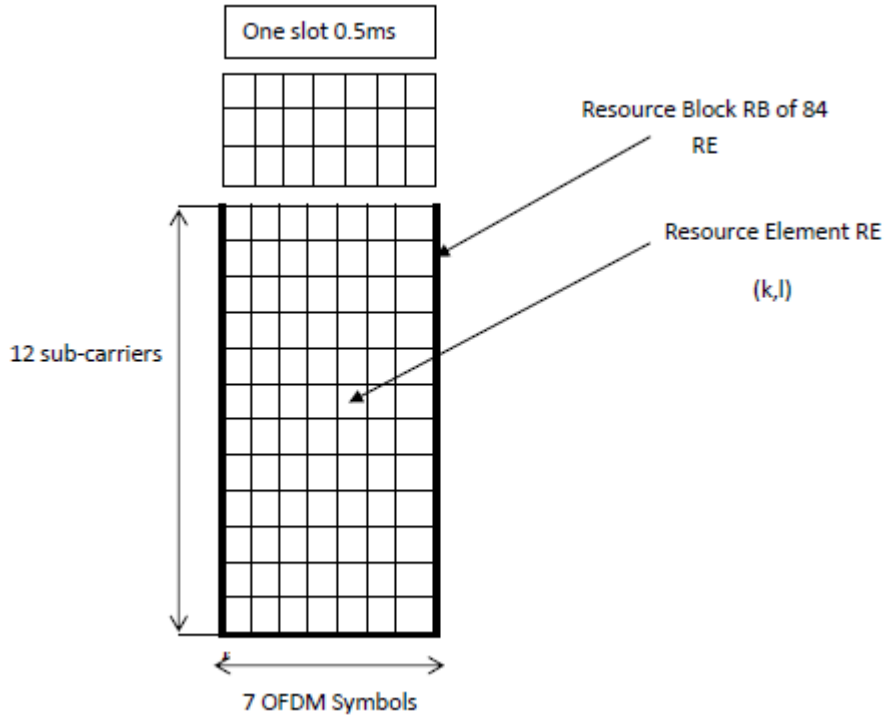

Figure 3.4: Downlink resource grid

domain, 12 sub carriers are grouped together to form a Resource Block (RB) occupying total 180 kHz in one slot duration as illustrated in figure 2.3. Thus the minimum allocated bandwidth to a UE is 180 KHz. In case of short CP, length a resource block contains 84 REs and for long CP the number of RE is 74. For multiple antenna schemes, there will be one resource gird per antenna. For all available bandwidths, the size of resource blocks is the same. Multiple resource blocks are assigned consecutively in the frequency domain to a UE in the uplink while dispersed, non-consecutive assignment, is done on the downlink.

The resource block (RB) is the basic element for radio resource allocation. The minimum size of radio resource that can be allocated is the minimum transmission time interval (TTI) in the time domain, that is, one subframe of 1 ms, corresponding to two resource blocks as shown in figure 3.5. The size of each resource block is the same for all bandwidths, which is 180kHz in the frequency domain. There are two kinds of resource blocks defined for LTE: physical and virtual resource blocks, which are defined for different resource allocation schemes as follows:

- Type-0 Allocation: In this type of allocation, several consecutive physical resource blocks (PRB) constitute a resource block group (RBG), and a resource allocation is done in units of RBGs. The allocated RBGs to a certain UE do not need to be adjacent to each other, which provides frequency diversity. The number of PRBs in each RBG depends on the system bandwidth.
- Type-1 Allocation: In this type of allocation, all the RBGs are grouped into a number of RBG subsets, and certain PRBs inside selected RBG subset are allocated to the UE. This type of resource allocation is more flexible and is able to provide higher frequency diversity, but it also requires a larger overhead.
- Type-2 Allocation: In this, PRBs are not directly allocated. Instead, virtual RBs are allocated, which are then mapped onto PRBs. A VRB is of the same size as a PRB and is of either localised type or distributed type.

3.3 LTE Downlink Reference Signal Structure

In order to carry out coherent demodulation in LTE down link, channel estimation is needed at the receiver end. In case of OFDM transmission known reference symbols are added into time frequency grid for channel estimation. These signals are called LTE Downlink reference signals. For time domain, reference symbols are slotted in the first and the third last elements of resource grid, where as reference signals are inserted over every six sub carriers in frequency domain. Furthermore, there is a frequency domain staggering of three sub-carriers between the first and second reference symbols. Therefore, there are four reference symbols within each Resource Block. Figure 3.5 show the structure of a RB and location of reference signals in normal CP mode with one transmitting antenna.

For an accurate channel estimation over entire gird and reducing noise in channel estimates, a two dimensional time frequency interpolation/averaging is required

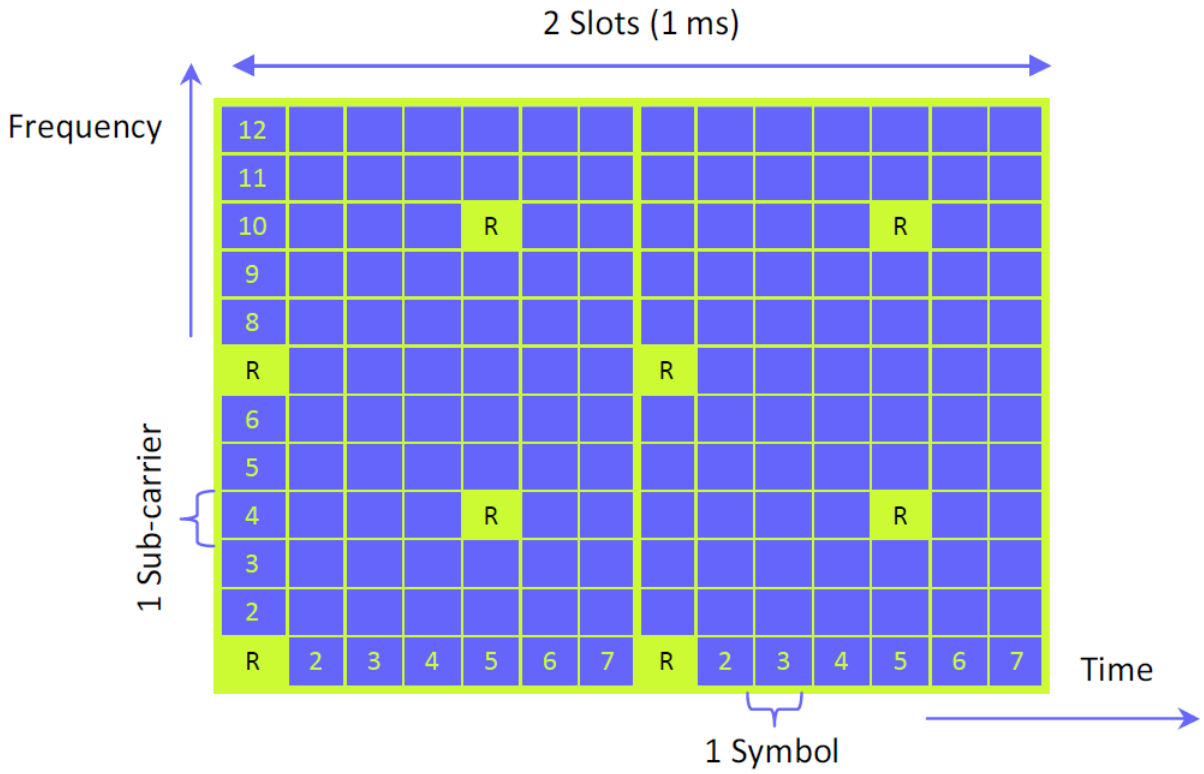

Figure 3.5: Reference symbols within a resource block, one antenna

over multiple reference symbols. One RS is transmitted from each antenna to estimate the channel quality corresponding to each path when a multiple antenna scheme is applied. In this case, RSs are mapped on different sub carries of resource grid for different antennas to refrain from interference. Resource elements used to transmit RSs from antenna 1 are not reused on antenna 2 for data transmission; these places are filled with zeros. Allocation of these reference symbols is shown in figure 3.6.

3.4 LTE Channel Models

The LTE channel models developed by 3GPP are based on the existing 3GPP channel models and ITU channel models. The extended ITU models for LTE are given the name of Extended Pedestrian-A (EPA), Extended Vehicular-A (EVA) and Extended Typical Urban (ETU). These channel models are classified on the

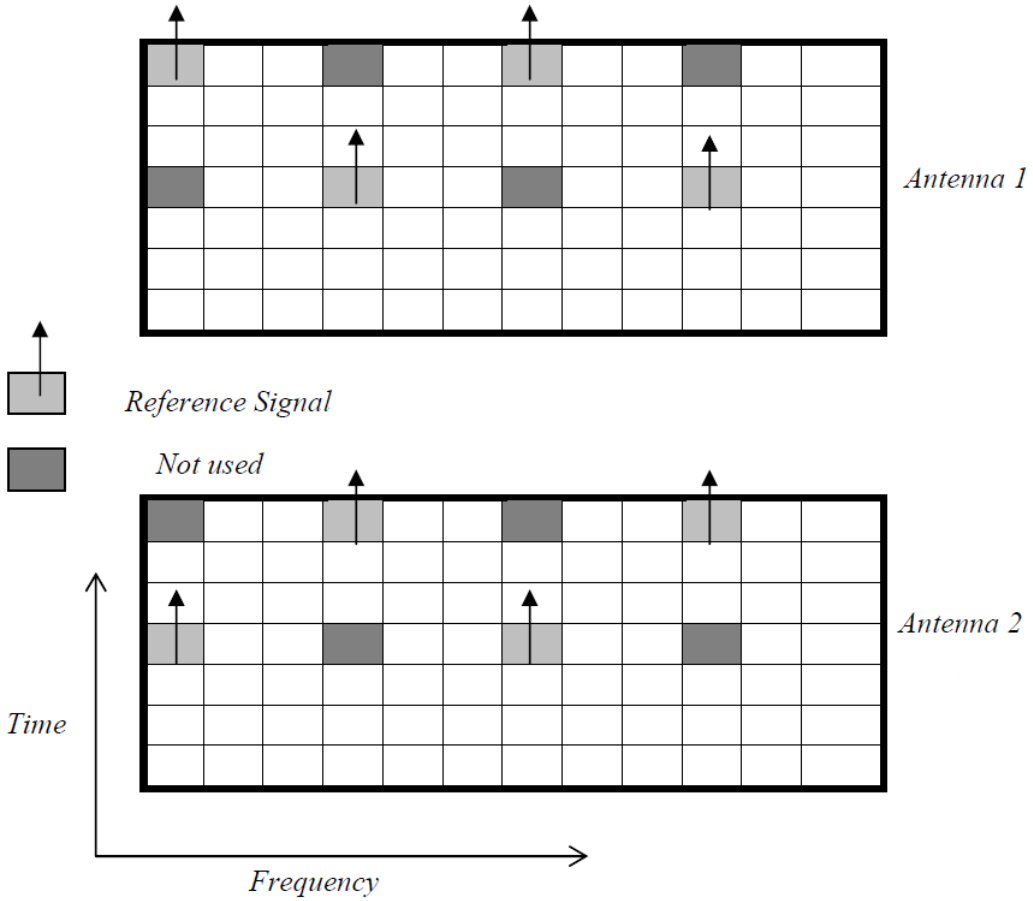

Figure 3.6: Allocation of RS for two antenna transmission

basis of low, medium and high delay spread where low delay spreads are used to model indoor environments with small cell sizes while medium and high delay spreads are according to typical urban GSM model. The power delay profile of these channel models are given in table 3.2, 3.4 and 3.5 respectively.

The above channel models are used in this work, mostly EVA, with classical Doppler spectrum. The maximum Doppler frequency used in our work is 10 Hz which ensures that the channel remains constant over 3 to 4 RBs in time.

	Tap No						
Average Power(dB)	0.0	-1.0	-2.0	-3.0	-8.0	-17.2	-20.8
Excess Delay(ns)	0.0	30	70	80	110	190	410

Table 3.2: Power Delay Profile for Extended ITU Pedestrian-A model

	Tap No								
Average Power(dB)	0.0	-1.5	-1.4	-3.6	-0.6	-9.1	-7.0	-12	-16.9
Excess Delay(ns)	0.0	30	150	310	370	710	1090	1730	2510

Table 3.3: Power Delay Profile for Extended ITU Vehicular-A model

3.5 MIMO MMSE Receiver

3.5.1 Introduction

MIMO schemes have been studied widely over the last few years and is considered as a suitable way to improve performance of wireless communication system. MIMO scheme can be split in two categories STC and SM. STC improves the reliability[1] of the communication system, while SM achieves a higher data rate [2] by transmitting independent data streams on different antennas simultaneously. With a ML detection, SM scheme has the maximum receive diversity order. The disadvantage of using ML decoding is its high computational complexity which can be overcome by using linear ZF or MMSE receiver.

LTE specifies usage of 2/4 antennas at BS and 2/4 antennas at UE. The receiver

	Tap No								
Average Power(dB)	-1.0	-1.0	-1.0	0.0	0.0	0.0	-3.0	-5.0	-7.0
Excess Delay(ns)	0.0	50	120	200	230	500	1600	2300	5000

Table 3.4: Power Delay Profile for Extended ITU Typical Urban model

employed is linear MMSE which optimally combines the signals from the receiving antennas to combat multipath fading and hence provide receive diversity. However, in addition, the MMSE receiver can also reduce the relative power of interfering signals or the CCI. When the interfering signals are present at both the antennas, the MMSE receiver achieves higher output SINR than maximal ratio combining (MRC) [3]. This type of MMSE based receiver, used in LTE, is known as IRC receiver and is effective in improving the cell-edge use throughput because it suppresses inter-cell interference.

3.5.2 System Model

In order to simplify the explanation of MIMO MMSE receiver, we consider a $1 \times N_r$ MIMO channel. The channel is assumed to be flat fading Rayleigh multipath channel. The channel between transmitting antenna and each receive antenna is assumed to be independent. For the j^{th} receive antenna, the transmitted symbol is multiplied by a randomly varying complex number $h_{1,j}$. As the channel under consideration is a Rayleigh channel, the real and imaginary parts of $h_{1,j}$ are Gaussian distributed having mean $\mu_{1,j} = 0$ and variance $\sigma^2_{1,j} = \frac{1}{2}$. It is assumed that the channel is known at the receiver. On the receive antenna, the noise$n$ has the

Gaussian probability density function with

$$f(x) = \frac{1}{\sqrt{2\pi\sigma^2}} e^{\frac{-(x-\mu)}{2\sigma^2}},\ \mu = 0,\ \sigma^2 = \frac{N_0}{2} \tag{3.1}$$

The received signal with in a given RB can be represented as

$$\bar{y} = \bar{h}x_d + \sum_{i=1}^{M} \bar{g}_i \bar{x}_i + \bar{n} \tag{3.2}$$

where $\bar{y}$ is the received signal vector with the baseband complex-valued entries of the signals received by j receive antennas, $\bar{h}$ is the channel vector consisting of the effective channel seen by the N_r receive antennas, $\bar{g}_i s$ are the channel vectors corresponding to M CCI signals and $\bar{n}$ is the thermal noise vector of variance $\frac{N_0}{2}$ per real dimension. The modulation alphabets of the desired signal and i^{th} CCI are denoted by x_d and x_i respectively.

3.5.3 MMSE Receiver

The decision metric z is obtained from the output $\bar{y}$ in (5) using MMSE filter W is given by,

$$z = W\bar{y} \tag{3.3}$$

From MMSE filter theory [4], the filter coefficients are given by,

$$W = R_{xy}R_{yy}^{-1} \tag{3.4}$$

where,

$R_{xy} = E[x_d \bar{y}^H] = E[|x_d|^2]\bar{h}^H = \bar{h}^H, \because E[|x_d|^2] = 1,$

where $(.)^H$ denotes the matrix Hermitian operation, and

$$R_{yy} = E[\bar{y}\bar{y}^H] = \bar{h}\bar{h}^H + R_{(i+n)},$$

where,

$$R_{(i+n)} = \sum_{i=1}^{M} E[|x_i|^2]\bar{g}_i\bar{g}_i^H + N_0 I \tag{3.5}$$

The interference-plus-noise covariance matrix $R_{(i+n)}$ is calculated by averaging the outer product of $(\bar{y_p} - \bar{h}x_p)$, at the pilot subcarriers that are scattered within the RB. The MMSE filter equations will become

$$W = \bar{h}^H[\bar{h}\bar{h}^H + R_{(i+n)}]^{-1} \tag{3.6}$$

By using matrix inversion lemma [5], the MMSE filter can be represented as:

$$W = (1 + \bar{h}^H R_{(i+n)}^{-1} h)^{-1} \bar{h}^H R_{(i+n)}^{-1} \tag{3.7}$$

The error covariance matrix at the output of the MMSE filter is $R_{ee} = (1 + \bar{h}^H R_{(i+n)}^{-1} h)^{-1}$. The scalar term in (10),

$$\alpha = 1 - R_{ee} = \frac{\bar{h}^H R_{(i+n)}^{-1} h}{(1 + \bar{h}^H R_{(i+n)}^{-1} h)}$$

represents the bias introduced by the MMSE filter [4]. This bias can be eliminated from the decision variable by scaling the MMSE filter with the bias term as:

$$\hat{x}_{MMSE} = (\alpha)^{-1} W \bar{y} \tag{3.8}$$

The decision variables are given to a conventional symbol demodulator, which in turn calculates the log-likelihood rations (LLR) for each bit. Note that the SINR at the output of the MMSE is given by:

$$SINR_{MMSE} = R_{ee}^{-1} = 1 + \bar{h}^H R_{(i+n)}^{-1} h$$

After bias-removal, the un-biased SINR at the output of MMSE is given by:

$$SINR_{U,\,MMSE} = SINR_{MMSE} - 1 = \bar{h}^H R_{(i+n)}^{-1} h \tag{3.9}$$

This type of MMSE receiver with N_r receive antennas can fully suppress $N_r - 1$ interferer sources [6]. Also, it is worth mentioning that the diversity order of this type of MMSE receiver is $N_r - M$. With N_r antenna array at the receiver, there are $N_r$degrees of freedom. M of these degrees of freedom are used to suppress interferer sources, leaving only $N_r - M$ left over for diversity gain. Thus suppression of each interfering source reduces the diversity order by one. Therefore there is a trade off between interference suppression and diversity gains.

4 Simulation Results

This chapter presents the simulated results, produced for conventional LTE MMSE receiver and DD MMSE receiver, using MATLAB.

4.1 Standard Parameters

We consider the following LTE downlink parameters in our work for performing MATLAB simulations:

- Channel models - ITU EPA, EVA and ETU with 10 Hz Doppler - known to the receiver.
- LTE frequency reuse - 1 mode.
- 1x2/ 1x3/ 1x4 MIMO system.
- Modulation - QPSK/ 16-QAM/ 64-QAM.
- Error Correction Codes - Turbo codes with rate = 1/2 (for BLER plots only).
- Bandwidth used is $10\,MHz$, where the number of sub-carriers is N = 1024 with sub-carrier spacing $\Delta f = 15\,kHz$. The sampling frequency is $15.36\,MHz$ and sampling time is $65.104\,ns$.
- Number of useful sub-carriers are 600 out of 1024. This excludes DC sub-carrier (to avoid interference) and 212+211 sub-carriers as guard band.
- Number of RBs = 50.

- LTE Type-1 frame structure with normal CP.
- Reference symbols are slotted-in over single RB as shown in figure 3.5.
- Number of interferer sources equals 1/ 2/ 3 with varying power levels of 0 dB/ -3dBs/ -10 dBs.
- Noise variance varying from 0.745 to 0.025.

4.2 MMSE Receiver

As discussed in section 3.5.2, the calculation of MMSE filter coefficients at the receiver requires the knowledge of interference+noise covariance matrix $R_{(i+n)}$. Since the actual $R_{(i+n)}$, as given by (9) in chapter 3, is not known at the receiver, hence the $R_{(i+n)}$ is calculated by averaging the outer product of $(\bar{y_p} - \bar{h}x_p)$ at the pilot sub-carriers (08 in numbers) that are scattered within the RB (figure 3.5). In this section, simulations results are presented for LTE MMSE receiver using single covariance matrix (conventional) and multiple covariance matrices formed by outer product of $(\bar{y_p} - \bar{h}x_p)$ at different pilot sub-carriers. The channel model used is EVA and the channel is assumed to remain constant over one RB duration and perfectly known to the receiver. For ease of notation, we would refer $R_{(i+n)}$ as 'covariance matrix' in rest of the thesis.

4.2.1 Conventional MMSE Receiver

Figure 4.1 shows the SER vs SNR plot of conventional MMSE receiver and compares its performance with the optimal case i.e. when the true covariance matrix is know at the receiver. The simulation is performed assuming the receiver has two antennas and there is only one transmit antenna. The data bits are modulated using QPSK and the receiver performs decoding after receiving one RB, during which time the channel is assumed to be constant and is perfectly known to the

receiver. In CCI simulations, only one dominant interferer, of same power (0 dB) as that of the desired signal is considered. The rest of the interference is considered as white noise, and SNR denotes signal to rest-of-the-interference+noise. As mentioned earlier, we observe that MMSE receiver with two antennas can fully suppress single interferer. We also observe that when noise variance becomes significantly lesser that interference power i.e. in high SNR region, the true covariance matrix case gives 6-7 dBs gain over conventional single covariance matrix case. Note that since the interferer channel is not known at the receiver, true covariance matrix cannot be formed at the receiver. Thus the aim of our work is to achieve as good performance as the true covariance case under different channel conditions and with different interference power levels.

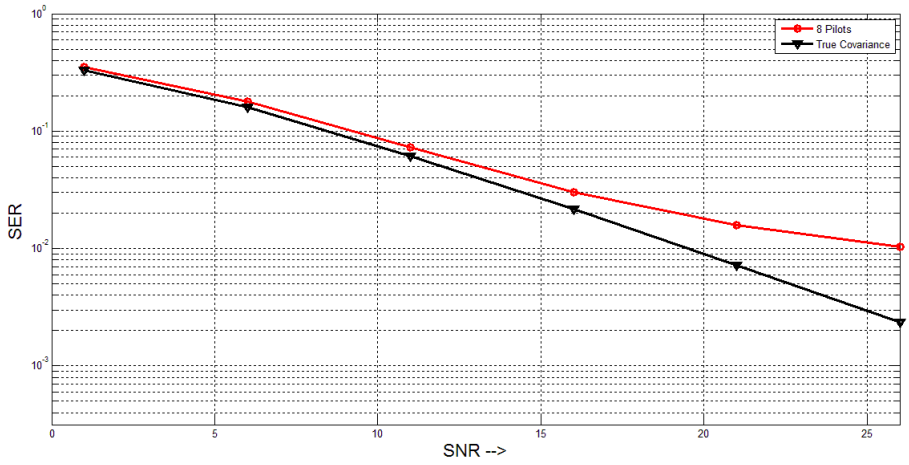

Figure 4.1: MMSE reciever- Conventional (08 Pilots) vs known True-covariance

Figure 4.2 shows the performance of conventional MMSE receiver with varying interference power level of an interferer. We observe that as the interference power decreases, the performance of the IRC receiver improves.

4.2.2 Multiple Covariance Matrices

The diagonals of $R_{(i+n)}$ represents the received interference power + noise power received at each antenna respectively. The interferer channel model is assumed

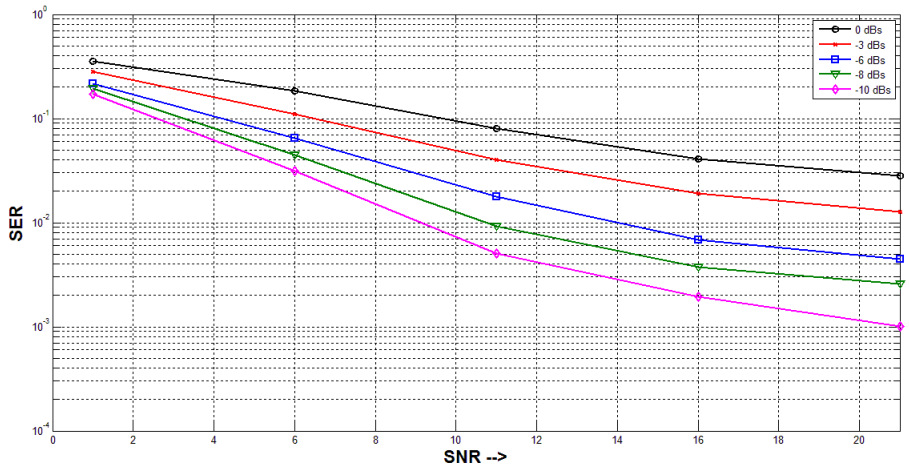

Figure 4.2: Conventional MMSE receiver performance under varying interference power level

to possess same behaviour as channel model between BS and UE. The channel is assumed to be constant over one RB time i.e the channel is fully correlated in time but not in frequency, though there is some correlation among the sub-carriers and the amount of correlation depends on the channel model considered. As mentioned earlier, the conventional receiver estimates the $R_{(i+n)}$ by averaging the outer product of $(\bar{y_p} - \bar{h}x_p)$ at pilot locations scattered in time and frequency within a RB. We propose a method of forming multiple covariance matrices instead of single averaged covariance matrix, in which we consider multiple covariance matrices by choosing different combinations of pilots scattered over RB. The division of RB is done only across sub-carriers and not across time since the channel is assumed to remain constant over one RB time. Figure 4.3 shows the performance comparison of single and multiple covariance matrices.

As shown in figure 3.2, in a RB structure there are 8 pilots. The pilot are located in 1st, 4th, 7th and 10th sub-carrier and for each sub-carrier there are two pilots located in time i.e. for 1st and 7th sub-carrier there are pilots in 1st and 8th OFDM symbol and for 4th and 10th sub-carrier pilots are located in 5th and 12th offend symbol. The division of pilot sub-carriers, to form multiple covariance matrix, is explained as follows:

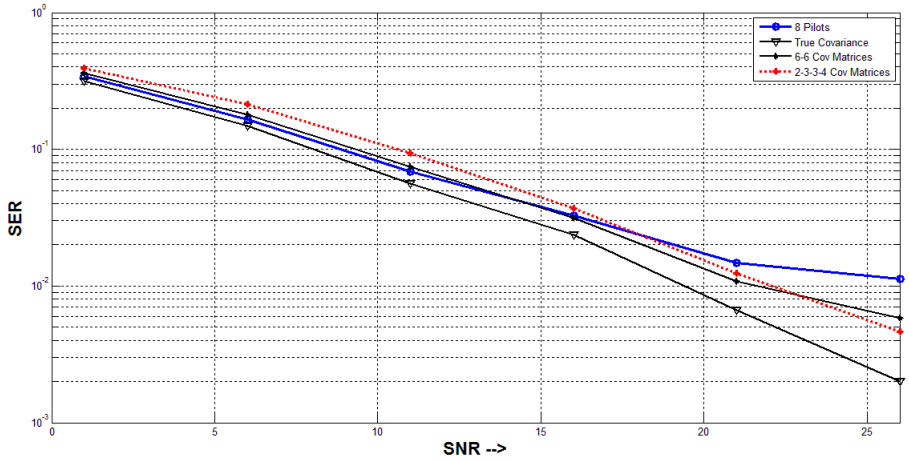

Figure 4.3: Multiple covariance matrices (0 dB interference), EVA

- 6-6 Covariance matrices: In this case, two covariance matrices are formed by dividing the RB is into two halves across sub-carriers i.e from sub-carrier 1 to 6 and 7 to 12. Each half has four pilots and the covariance matrix at each half is formed by averaging outer product of $(\bar{y_p} - \bar{h}x_p)$ at these four pilot locations. Thereafter, the symbols in each half are decoded by the covariance matrix of the respective half.

- 2-3-3-4 Covariance matrices: In this case, four covariance matrices are formed by considering all four sub-carrier separately. Each sub-carrier has two pilots in time and hence each covariance matrix is averaged by outer product of $(\bar{y_p} - \bar{h}x_p)$ at these two pilot locations. Thereafter, the first covariance matrix decodes symbols in first two sub-carriers, the second covariance matrix decodes symbols in next three sub-carriers, the third covariance matrix decodes symbols in next three sub-carriers and the fourth covariance matrix decodes symbols in last four sub-carriers.

It is worth mentioning that performance of IRC receiver depends mainly on accuracy of covariance matrix and channel estimation. Since we have assumed the perfect channel knowledge, the accuracy of covariance matrix is the main factor upon which the performance of the MMSE receiver depends. The accuracy of

covariance matrix depends on accuracy of determining noise variance and interference power. Ideally, when there is no noise present, the accuracy of covariance depends on accuracy of determining interference power which differs from subcarrier to subcarrier. In such cases, we should always consider 2-3-3-4 case i.e. separate covariance matrices because the channel varies across sub-carriers and is fully correlated in time. Also, in no noise condition one pilot per sub-carrier is sufficient for determining covariance matrix and no further averaging is required. However, since the noise is ever present, we have mainly two cases to deal with: first when the noise variance is comparable to interferer's power, and second when the noise variance is very very small as compared to interferer's power. When the noise power is very very low (1/60 times approx for EVA) as compared to interference power, we should consider separate covariance matrix for each sub-carrier. Because in this case interferer is dominating and lesser averaging (two for each sub-carrier) of covariance matrices is sufficient to accurately estimate the comparatively low noise component and hence the covariance matrix. It is reiterated that in no noise condition, which is the ideal condition, averaging of covariance matrix is not required and separate covariance matrix at pilot sub-carriers gives accurate interference power estimate and hence covariance matrix. However, when noise power is $> 1/60$ times (for EVA) the interference power, we need more averaging to accurately determine noise variance. In such cases, better noise variance estimate can be obtained by considering more pilot subcarriers for averaging of covariance matrices. Hence, in these cases averaging can be performed over pilots in the nearby/ all sub-carriers. It should be noted that averaging over pilots in different subcarriers compromises the accuracy of determining interference power which varies from subcarrier to subcarrier.

From the results shown in figure 4.3 and 4.4, the performance of single covariance matrix supersedes the other two cases at low SNRs i.e. when the noise power comparable to the interferer power. Whereas at high SNR region, when the noise

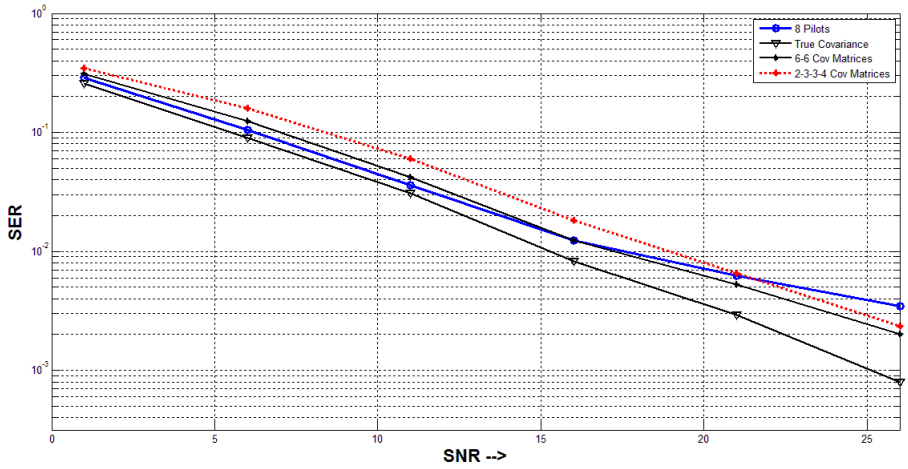

Figure 4.4: Multiple covariance matrices (-3 dBs interference), EVA

power is very small as compared to the interferer power, the 2-3-3-4 case has best performance and the single covariance has the worst SER. Since in 6-6 case, the covariance matrices are averaged over four pilots, they outperforms other schemes in the mid SNR region where noise variance is neither too low nor too high as compared to interference, and hence four averages are optimal to accurately determine covariance matrices. It is worth mentioning that if the channel is not highly frequency selective e.g. EPA, there is high frequency correlation among sub-carriers, the averaging can be performed across the sub-carrier too which would give better noise variance estimate. Since noise variance in each sub-carrier is same, single covariance matrix would estimate covariance matrix more accurately as compared to multiple covariance matrices.

4.3 Decision Directed MMSE Receiver

We have seen that how averaging of covariance matrices improves the accuracy in determining noise variance and hence the covariance matrix. The main idea behind decision directed MMSE receiver is to include the data points (REs with data) in averaging the covariance matrix. However, the data points can be included only after making the decision at these data points by any of the methods mentioned

above. Since the decisions made need not always be accurate at all the data points, considering all the data points for averaging of covariance matrix may not be a good option.

Thus, including only those data points which are relatively close to the transmitted constellation points after filtering, may prove to be a better option. To verify this, we have performed simulations for QPSK, 16-QAM and 64-QAM which are shown in figure 4.5, 4.6 and 4.7 respectively.

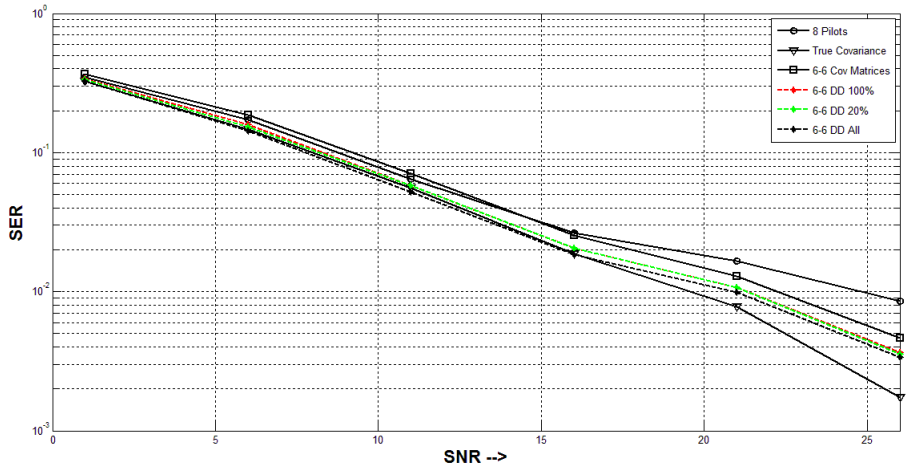

Figure 4.5: DD MMSE: QPSK, 0 dB interference, EVA

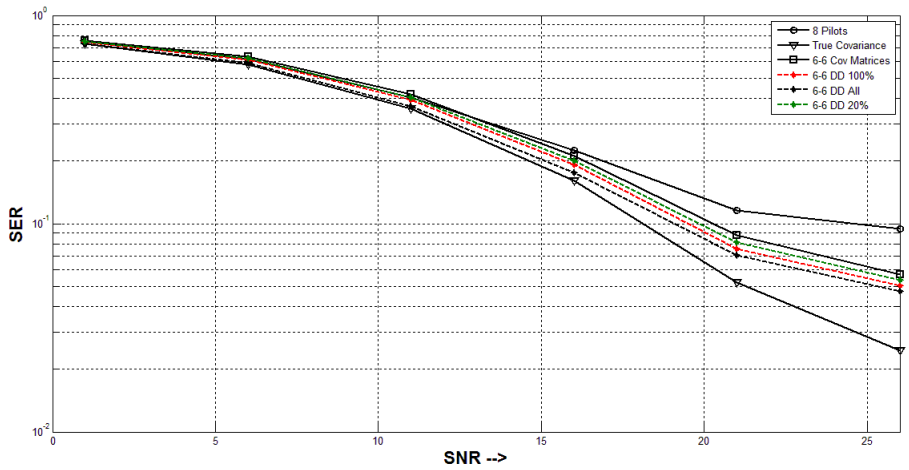

Figure 4.6: DD MMSE: 16-QAM, 0 dB interference, EVA

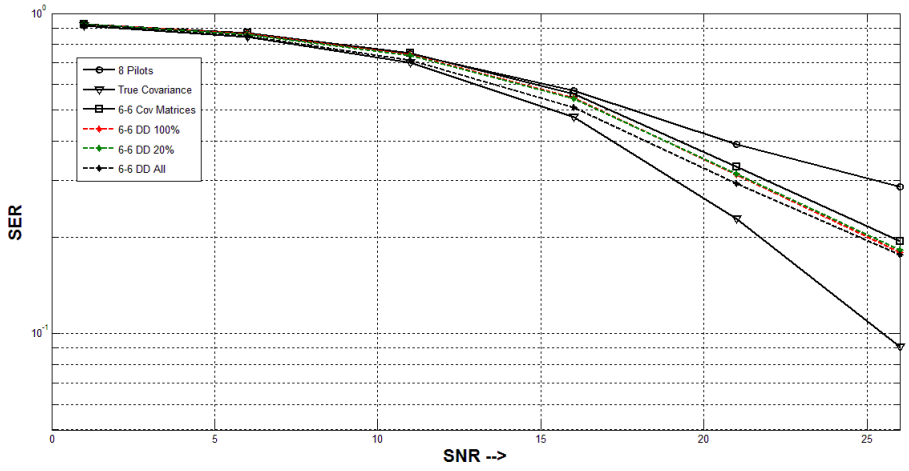

Figure 4.7: DD MMSE: 64-QAM

In the simulations, data points are obtained by initially making decisions using 6-6 covariance matrix and these data points are further used for averaging covariance matrices (6-6) and making decisions again. In the figures above, 6-6 DD 100 % represents that all the data points are considered for averaging of 6-6 DD covariance matrices. 6-6 DD 20 % indicates that only those decisions are considered for averaging, which are within 20 % boundary of the transmitted constellation points i.e close to the transmitted constellation and are more likely of being correct. 6-6 DD All refers to the ideal case when all true decisions are fed for averaging and is plotted for comparison purpose only. Figure 4.5 shows that 6-6 DD 20 % has 0.05 dB more gain than 6-6 DD 100% which is marginal. But as the modulation order increases, as shown in figure 4.6 and 4.7, the 6-6 DD 100% performs better because of denser constellation. From above figures, we also observe that over the range of SNR and different modulation schemes, there is only 0.1-0.4 dBs difference between 6-6 DD 100% and 6-6 DD All. Therefore it is appropriate to consider all the decisions, whether right or wrong, in all cases for calculation of covariance matrices.

Figure 4.8 and 4.9 shows the plots for 6-6 DD 100% case with 0 dB interference power and -10 dBs interference power. We observe that in both the cases, the DD

method outperforms single covariance method with the gain ranging from 1 dB to 6 dBs.

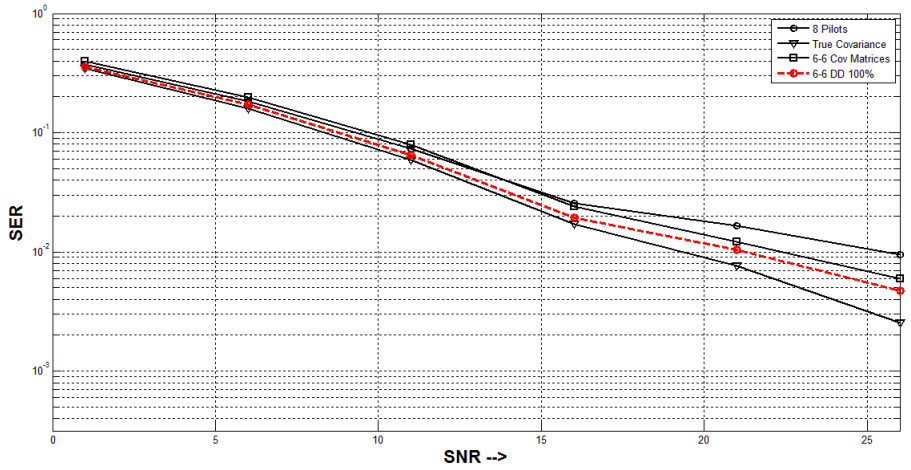

Figure 4.8: DD MMSE: QPSK, 0 dB interference, EVA

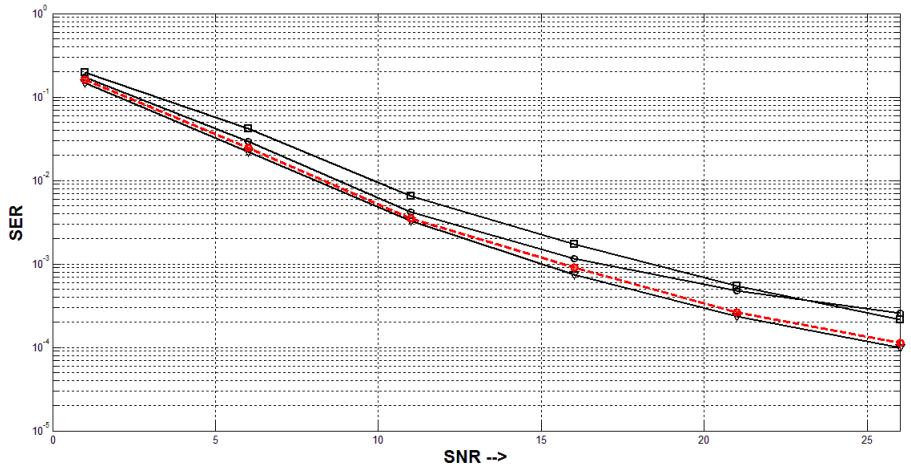

Figure 4.9: DD MMSE: QPSK, -10 dBs interference, EVA

4.4 Multiple Covariance Matrices DD MMSE

Since we have both data points and pilot carriers, we can have different combination of covariance matrices. We now consider forming 12 DD matrices, one each for a sub-carrier averaged over 14 offend symbols, and compares its performance with

single DD covariance matrix averaged over 168 REs. The comparison is shown in figure 4.10.

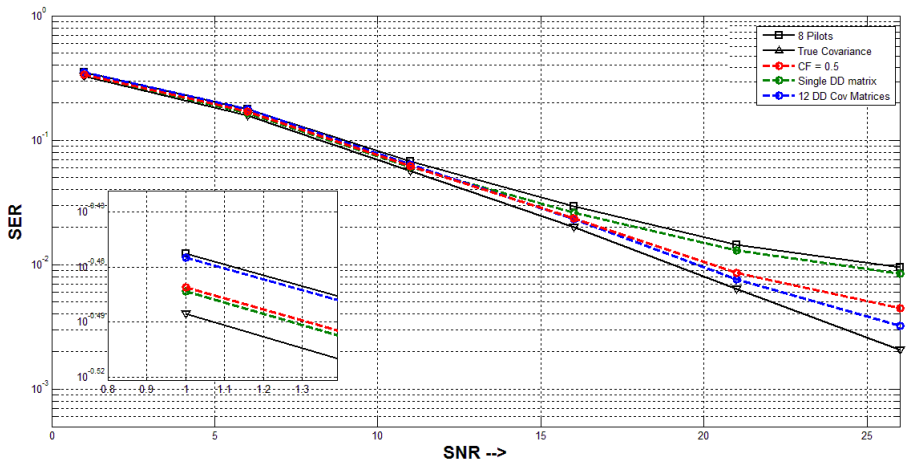

Figure 4.10: Single and multiple DD covariance matrices, 0 dB interference, EVA

We observe that in higher SNR region the 12 DD covariance matrix outperforms single DD covariance matrix and vice a versa because of the same reasons mentioned earlier. It is worth mentioning that both the schemes achieve gain over conventional 08 pilot covariance matrix based scheme. The performance of the receiver can further be enhanced by adaptively choosing between 12 DD and 1 DD covariance matrix based schemes. The choice can be made based on the fact that interferer channel has full correlation in time and some correlation in frequency which depends on the channel model.

The coherence bandwidth of the channel specifies the correlation among subcarriers. The coherence bandwidth can be specified based on the correlation coefficient of signals separated in frequency. Correlation coefficient values of 0.9 or 0.5 are generally used to define the coherence bandwidth. If the correlation coefficient between the amplitudes of the signals at two different frequencies is set to 0.9, the

coherence bandwidth is estimated by the following expression:

$$B_{cf} = \frac{1}{50\sigma_{rms}} \tag{4.1}$$

where, σ_{rms} is the important parameter called rms delay spread of the channel. On the other hand, if we consider a correlation coefficient of only 0.5, the coherence bandwidth is estimated by the following expression:

$$B_{cf} = \frac{1}{5\sigma_{rms}} \tag{4.2}$$

The LTE channel has standard rms delay spread of 991 nsec. Thus the coherence bandwidth of LTE channel can vary between 25 KHz to 200 KHz depending on the correlation coefficient used. With correlation coefficient of 0.5, the coherence bandwidth of LTE channel is 200 KHz i.e 12 to 13 sub-carriers are assumed to be coherent.

The method of choosing between 1 DD and 12 DD is explained as follows:

- Calculate DD covariance matrix for each sub-carrier i.e. 12 DD matrices.
- Compare the first diagonal element of all 12 matrices. The ratio of minimum to maximum of the 12 values should not be lesser than 0.5.
- If the ratio is lesser than 0.5, choose 1 DD scheme else choose 12 DD scheme.
- Perform this operation for the second diagonal elements of 12 matrices and so on.

As stated earlier, in low SNR region the noise variance is high and comparable to interference power. Averaging of covariance matrix along 14 offend symbols in time, does not accurately estimate the noise variance/ covariance matrix for each

sub-carrier. Thus there is lesser correlation among respective diagonal elements of the 12 covariance matrices. However, when the noise variance is lesser as compared to interference power in high SNR region, the correlation among sub-carriers is evident and the above test chooses 12 DD scheme. The performance of this method is shown in figure 4.10, with legend 'CF=0.5', where CF stands for correlation factor. It is observed that in lower SNR regions, it chooses 1 DD scheme for almost 90% of the iterations. In high SNR regions, it chooses 12 DD scheme for almost 85-90 % of the iterations. Figure 4.11, 4.12 and 4.13 shows the performance of this method in ETU, EPA and a random exponential channel models. Figure 4.14 shows the performance of single and multiple DD covariance matrices when higher modulation (16 QAM) schemes are employed.

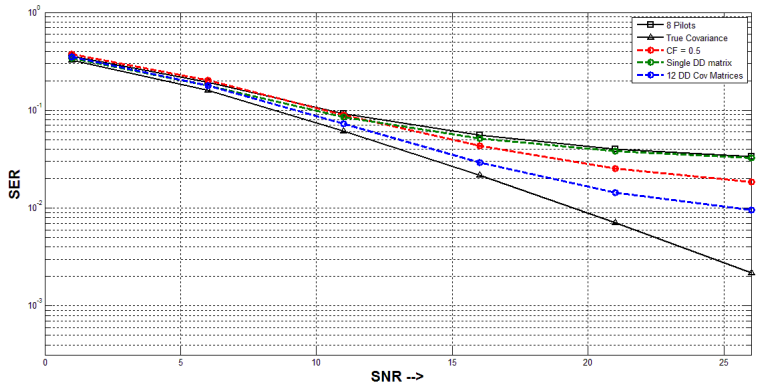

Figure 4.11: Single and multiple DD covariance matrices, 0 dB interference, ETU

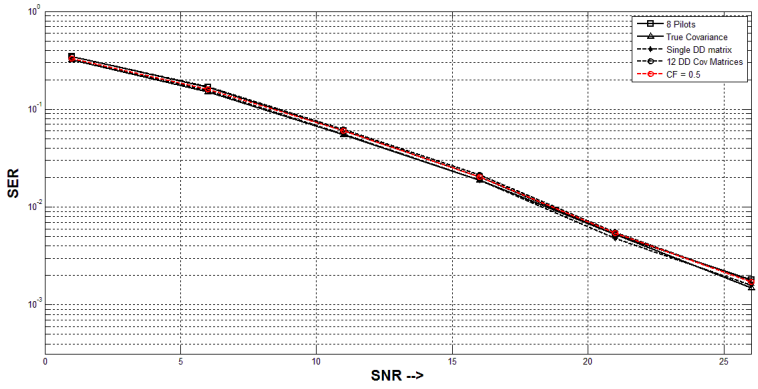

Figure 4.12: Single and multiple DD covariance matrices, 0 dB interference, EPA

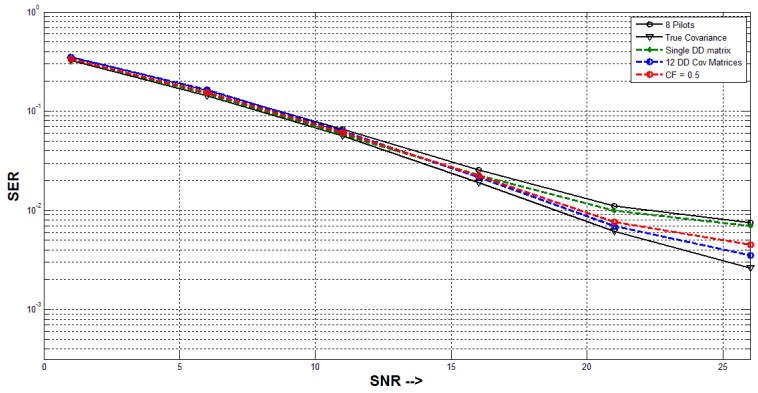

Figure 4.13: Single and multiple DD covariance matrices, 0 dB interference, Exponential PDP

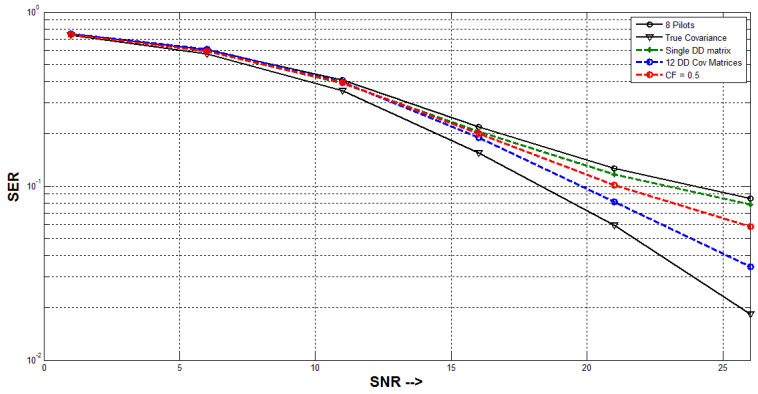

Figure 4.14: Single and multiple DD covariance matrices, 0 dB interference, 16 QAM

We observe that the performance of 1 DD and 12 DD schemes outperforms conventional MMSE receiver scheme in all channel conditions and modulation schemes. However, the gain offered by proposed schemes over conventional method is more in highly selective channels (EVA and ETU) as compare to benign ones (EPA and EPB). Also, the method used for choosing the matrices adaptively performs fairly well in all channel conditions and modulation schemes.

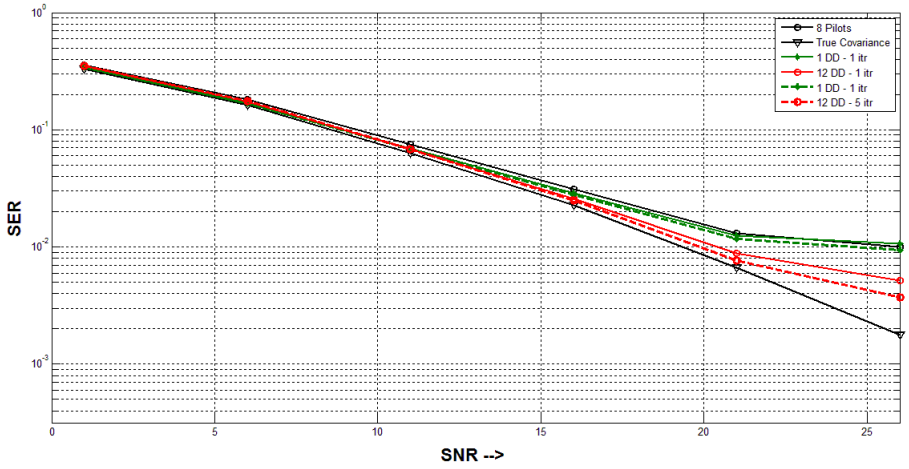

Figure 4.15: Iterations in DD Schemes, 0 dB interference, EVA

Figure 4.15 shows the performance improvement of iterative DD scheme over single iteration DD scheme. In iterative DD scheme, once the decisions are made using DD covariance matrices, the new decisions are used to calculate new set of covariance matrices and thus making decisions based on these new set of covariance matrices. Figure 4.15 compares five iterations of such loop with a single iteration DD scheme. It is observed that by iteratively making decision improves the performance of DD schemes.

Figure 4.16 and 4.17 shows the performance of DD MMSE receiver in three and four receive antennas case respectively. The receiver with three interferer sources can suppress two dominant interferer sources which can be seen in figure 4.16. The receiver equipped with four antenna can suppress three dominant interferer sources which is evident in figure 4.17. In both the cases, all interferer sources are assumed to have 0 dB power each.

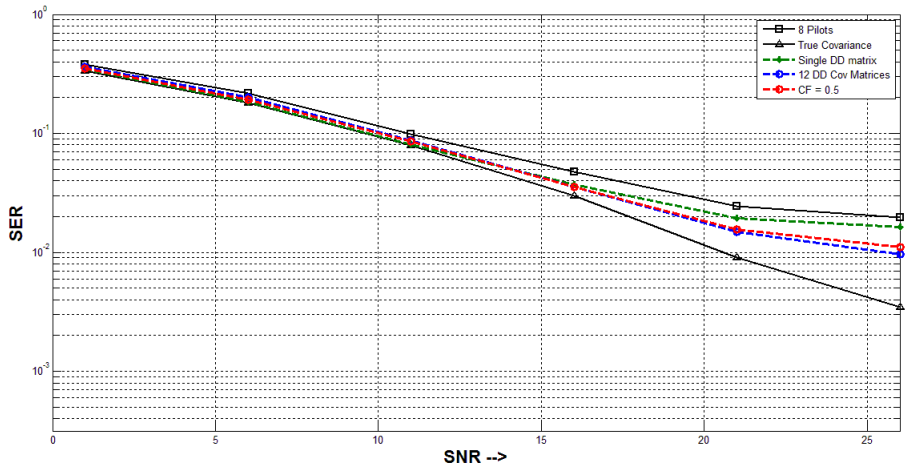

Figure 4.16: DD MMSE - Three receive antennas, two 0 dB interferer sources, EVA

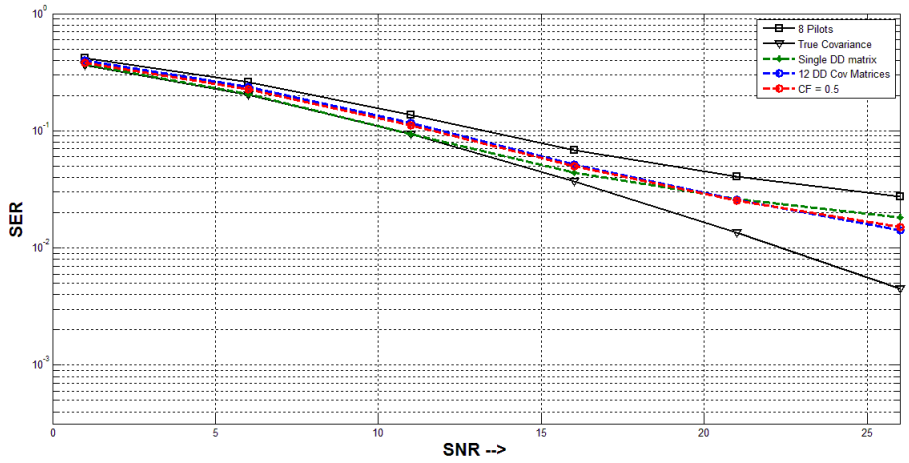

Figure 4.17: DD MMSE - Four receive antennas, three 0 dB interferer sources, EVA

4.5 BLER performance of MMSE Receiver

In this section we simulate for BLER performance of single and multiple covariance matrices techniques. A block is said to be in error if even a single bit in the block is in error. In the simulations, the data bits are first coded with code rate of 1/2, then modulated using QPSK, transmitted over channel, equalized with MMSE filter and then decoded using a turbo decoder. The coding is applied over single RB in the

simulations, but can be applied over multiple RBs in practice. The length of the code increases as the coding is done over multiple RBs and due to superior performance of large length turbo codes over smaller length turbo codes, better performance is achieved. Further, if multiple RBs are spread over entire frequency range, i.e. they are not contiguous, frequency diversity would further improve the BLER performance. Figure 4.18 and 4.19 shows the performance comparison of varying length turbo codes in AWGN channel and LTE EVA channel with 0 dB interference respectively. In figure 4.19 the comparison is made for coding over single RB, 4 contiguous RBs (2 in frequency and 2 in time) and six contiguous RBs (3 in frequency and 2 in time). We observe that coding over number of blocks improves the BLER performance.

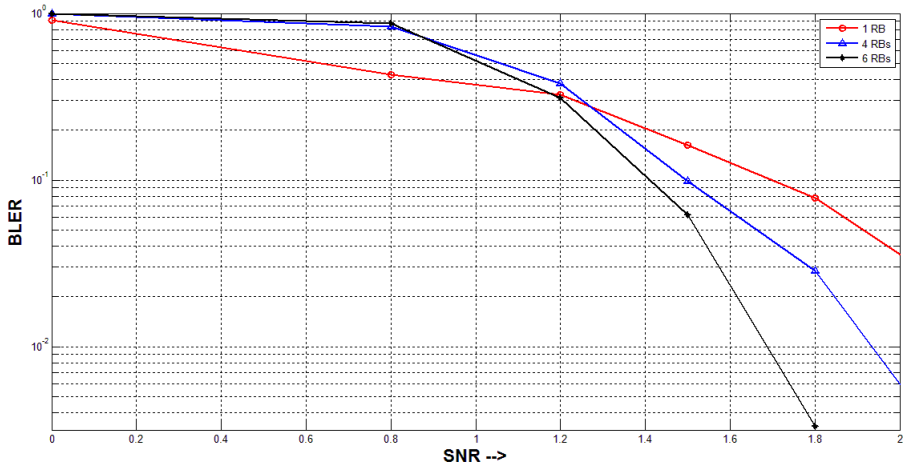

Figure 4.18: BLER comparison for varying length codes in AWGN, QPSK

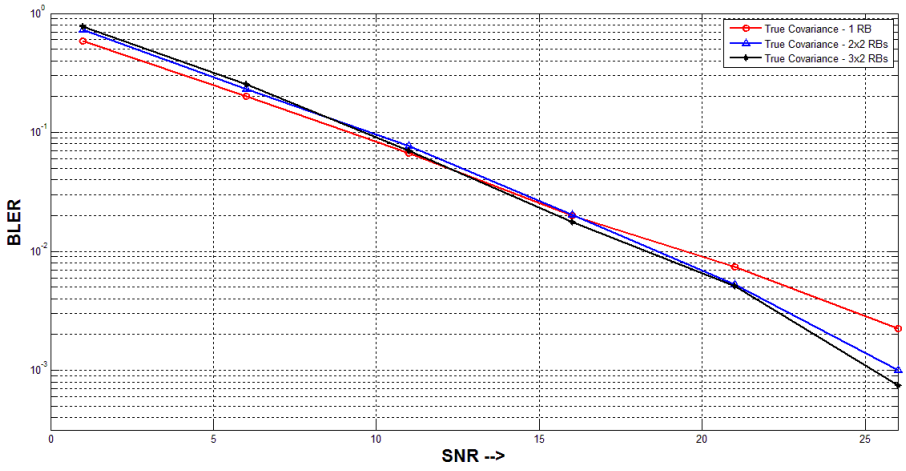

Figure 4.19: BLER comparison of varying length codes in EVA with 0dB interference

Figure 4.20 and 4.21 shows the turbo coded BLER performance of single DD matrix and 12 DD covariance matrices schemes for QPSK and 16-QAM modulation respectively. The plots also give the performance of the method chosen for adaptively choosing between 1 DD and 12 DD schemes. We observe that the inclusion of decisions made, post error correction by turbo codes, in evaluating covariance matrices significantly improves the performance of 12 DD scheme at higher SNRs, especially for QPSK.

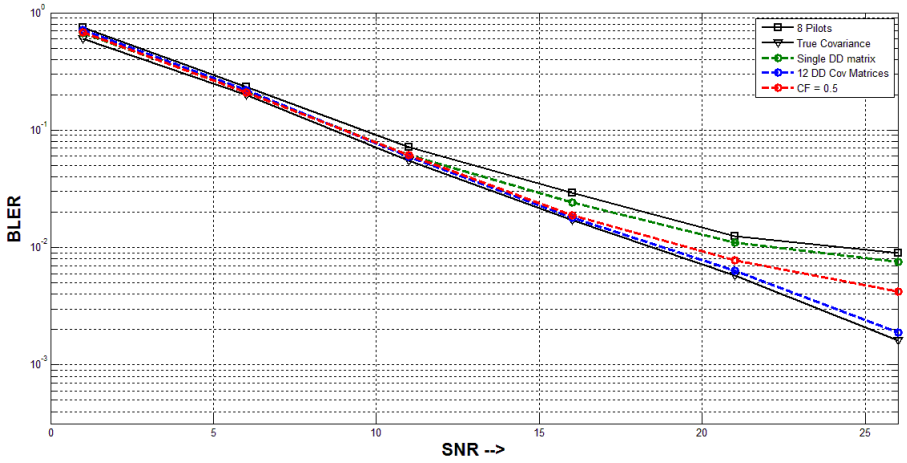

Figure 4.20: BLER comparison of single and multiple DD covariance matrices-QPSK, 0 dB interference, EVA

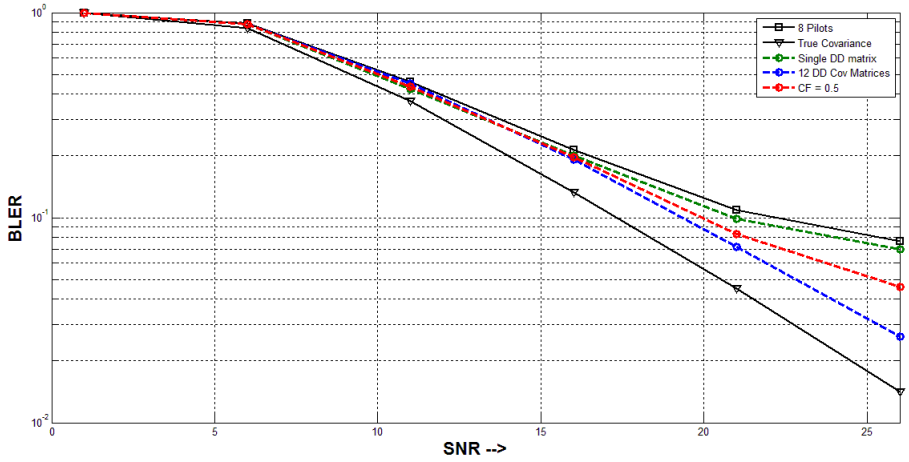

Figure 4.21: BLER comparison of single and multiple DD covariance matrices-16QAM, 0 dB interference, EVA

5 Conclusion

In this thesis, the performance of IRC receiver used in LTE downlink has been investigated under different types of LTE channel models and different modulation schemes. The IRC receiver based on MMSE is sensitive to accuracy of interference-plus-noise covariance matrix which is obtained by known RS. We have proposed a new scheme of forming multiple interference-plus-noise covariance matrices within a RB instead of using a conventional receiver which employs single noise-plus-covariance matrix. The performance of single and multiple covariance matrices was investigated under varying powers of interfering source and varying noise variance. Simulated results show that the performance of single and multiple matrices schemes is a function of ratio of noise power to interference power as well as the frequency selectivity of the channel. Among multiple covariance matrices schemes and single covariance matrix scheme, no single scheme gives optimal performance in all the cases.

In order to improve the performance of pilot aided IRC/ MMSE receiver, we have proposed a decision directed (DD) scheme. This new scheme includes the data points, obtained by decisions made by conventional method, in determining the noise-plus-covariance matrix. In this decision directed scheme, we considered two cases: forming single DD covariance matrix and forming 12 DD covariance matrices i.e. one for each subcarrier. Both these schemes outperforms conventional pilot based single covariance method in all channel conditions and modulation schemes. The performance comparison of these two schemes shows that no single scheme

is optimal for all the cases. Hence a method of adaptively choosing one of these two schemes is proposed which is based on correlation factor of channel coherence bandwidth. The BLER and SER performances of single DD scheme, 12 DD scheme and the adaptive scheme has been investigated under varying channel conditions, modulation schemes, interferer source power levels and number of interfering sources. The performance of DD schemes outperforms the conventional single covariance matrix based scheme in all the cases. These gain achieved by proposed DD schemes over the conventional method varies from case to case and is maximum in severe channel conditions and high interference power to noise ratio.

Bibliography

[1] S. M. Alamouti, "A simple transmit diversity technique for wireless communications," *IEEE J. Select. Areas Commun.*, vol. 16, pp. 1451 – 1458, October 1998.

[2] G. Foschini and M. Gans, "On limits of wireless communication in a fading environment when using multiple antennas," *Wireless personal communnications*, pp. 311 – 335, March 1998.

[3] J. H. Winters, "Optimum combining in digital mobile radio with cochannel interference," *IEEE Transactions on Vehicular Technology*, vol. VT-33, No.3, August 1984.

[4] J. Cioffi, *EE:379 Stanford Class Notes.* [Online]. Available: http://www.stanford.edu/class/ee379a/

[5] R. A. Horn and C. R. Johnson, "Matrix analysis," *Cambridge University Press, 1990.*

[6] J. H. Winters and J. Salz, "Upper bounds on bit error rate of optimum combining in wireless systems," *IEEE Trans. Commun.*, pp. 1619 – 1624, Dec 1998.